

M S U H E P -041008
 hep-ph/0410181

B -m eson signatures of a
 Supersym m etric U (2) avor m odel

Shrihari G opalakrishna ^y and C .P. Yuan^z

D epartment of P hysics and A stronomy,
 M ichigan State U niversity,
 East Lansing, M I 48824, U SA .

(D ated: M ay 23, 2019)

A bstract

We discuss B -m eson signatures of a Supersym m etric U (2) avor m odel, w ith relatively light (electroweak scale m asses) third generation right-handed scalars. We impose current B and K m eson experimental constraints on such a theory, and obtain expectations for $B_d \rightarrow X_s$, $B_d \rightarrow X_s \gamma$, $B_d \rightarrow X_s \pi^+$, $B_d \rightarrow K_s$, $B_s B_s$ m ixing and the dilepton asym m etry in B_s . We show that such a theory is compatible w ith all current data, and furthermore, could reconcile the apparent deviations from Standard M odel predictions that have been found in some experiments.

Current address: D ept. of P hysics and A stronomy,
 N orthwestern U niversity, E vanston, IL - 60208, U SA .

^yE lectronic address: shri@ northwestern.edu

^zE lectronic address: yuan@ pa m su.edu

I. INTRODUCTION

The Standard Model (SM) of high energy physics suffers from the gauge hierarchy problem and the flavor problem. The first is the fine tuning required to maintain a low electroweak mass scale (M_{EW}) in the theory, in the presence of a high scale, the Planck Scale (M_P). The second problem is a lack of explanation of the mass hierarchy and mixings of the quarks and leptons.

Supersymmetry (SUSY) eliminates the gauge hierarchy problem by introducing for each SM particle, a new particle with the same mass but different spin. For example, for each SM quark/lepton a new scalar (squark/slepton), and for each SM gauge boson a new fermion (gaugino), is introduced. If SUSY is realized in nature, the fact that we do not see such new particles, we believe, could be because SUSY is spontaneously broken, making the superpartners heavier than the mass ranges probed by experiments. Owing to a lack of understanding of how exactly SUSY is broken, a phenomenologically general Lagrangian, for example, the Minimal Supersymmetric Standard Model (MSSM), is usually considered to compare with data. Various experimental searches have placed constraints on the masses and couplings in the MSSM.

Attempts have been made to address the flavor problem by proposing various flavor symmetries. In a supersymmetric theory, a flavor symmetry in the quark sector might imply a certain structure in the scalar sector, leading to definite predictions for flavor changing neutral current (FCNC) processes on which experiments have placed severe constraints. In the literature, a lot of attention has been devoted toward analyzing the minimal flavor violation (MFV) scenario, in which the scalar flavor structure is aligned with the quark sector so that the two are simultaneously diagonalized. In MFV, the CKM matrix describes the flavor changing interactions in the supersymmetric sector as well, and the only CP violating phase is the one in the CKM matrix. In this work, we do not assume such an alignment, and we will consider non-minimal flavor violation (NMFV), which we treat as a perturbation over the MFV case.

In this paper we wish to explore in what form a supersymmetric extension of the SM,

with a $U(2)$ flavor symmetry, could influence K and B physics observables. We thus restrict ourselves to the quark and scalar-quark (squark) sectors. We consider an "effective supersymmetry" [1] framework, with heavy (TeV scale) first two generation squarks, in order to escape neutron electric dipole moment (EDM) constraints. This allows the possibility of having large CP violating phases in the squark sector. We consider a supersymmetric $U(2)$ theory [2, 3], impose recent K and B meson experimental constraints and obtain predictions for $B_d \rightarrow X_s \bar{g}$, $B_d \rightarrow X_s \bar{s}^+$, $B_d \rightarrow K_s \bar{B}_s$ mixing and the dilepton asymmetry in B_s . Though we consider a specific flavor symmetry, namely $U(2)$, our conclusions would hold for any model with a sizable off-diagonal 32 element in the squark mass matrix.

Some B physics consequences in a supersymmetric $U(2)$ theory have been considered in Ref. [3]. Large flavor effects in B decays have been carefully analyzed in Ref. [4], but for simplicity we will restrict ourselves to the case when $\tan\beta$ is not too large. Other work along similar lines, though in more general contexts, have been presented in Ref. [5, 6, 7, 8]. In this work we will include all dominant contributions to a particular observable in order to include interference effects between various diagrams. This has not always been done in the literature. We will then study the implications of recent data from the B -factories, including the $b \rightarrow s$ penguin decay mode $B_d \rightarrow K_s$ which shows a slight deviation from the SM prediction.

The paper is organized as follows: In Section II we specify the supersymmetric $U(2)$ theory we will work with, and the choices we make for the various SUSY and SUSY breaking parameters. In Sections III and IV we consider $S = 2$ (Kaon mixing) and $B = 2$ ($B_d \bar{B}_d$ and $B_s \bar{B}_s$ mixing) FCNC processes, respectively. In Section V we will consider the implications of such a theory to $B = 1$ FCNC processes, namely $B_d \rightarrow X_s \bar{g}$, $B_d \rightarrow X_s \bar{s}^+$ and $B_d \rightarrow K_s$. We conclude in Section VI. We give details of various squark mixings and their diagonalization in Appendix A, and collect loop functions that we will need in Appendix B.

II. SUPERSYMMETRIC U(2)

A. The Model

The supersymmetric model that we will discuss is as described in Ref. [3], with the first and second generation superfields ($a, a=1,2$) transforming as a U(2) doublet while the third generation superfield (b) is a singlet. The most general superpotential can be written as :

$$W = \frac{1}{M} H^a + \frac{a}{M} H^{ab} + \frac{ab}{M} H^b + \frac{a}{M^2} H^{ab} + \frac{b}{M^2} H^{ab} + \frac{S^{ab}}{M} H^a H^b + H_u H_d; \quad (1)$$

where M is the cut-off scale below which such an effective description is valid, the i are $O(1)$ constants, and three new U(2) tensor fields are introduced: a a U(2) doublet, ab a second rank antisymmetric U(2) tensor and S^{ab} a second rank symmetric U(2) tensor. The parameter v could be complex and we allow for this possibility. Following Ref. [3], we assume that U(2) is broken spontaneously by the vacuum expectation value (VEV)^y [3]

$$h^a_i = \frac{0}{v}; \quad {}^D H^{ab} = v^{ab}; \quad {}^D S^{11;12;21} = 0; \quad {}^D S^{22} = v; \quad (2)$$

with $v=M=0.02$ and $v=0.004$, in order to get the correct quark masses. These VEV's lead to the quark mass matrix given by (we show only the down quark mass matrix after the $SU(2)_L$ is broken by the usual Higgs mechanism)

$$L \quad \begin{matrix} \bar{d}_R & s_R & b_R \end{matrix} M \quad \begin{matrix} \bar{d}_L & s_L & b_L \end{matrix} + h.c.; \quad (3)$$

In the superpotential each term encodes the "vertical" gauge symmetry, which, at the weak scale, is $SU(3) \times SU(2) \times U(1)$. Thus (i, j labels generations),

$$i H_j = {}^u Q_i U_j^c H_u + {}^0_u U_i^c Q_j H_u + {}^d Q_i D_j^c H_d + {}^0_d D_i^c Q_j H_d + (\text{Lepton sector});$$

^y The dynamical mechanism by which this VEV is generated is left unspecified. In general, S^{22} can be different from h^a_i , but for simplicity we will assume that they are the same. Also for simplicity, we take v^0 to be real.

$$M_d = v_d \begin{pmatrix} 0 & 0 & 1 \\ 1 & 0 & 0 \\ 0 & 1 & 0 \\ 0 & 0 & 1 \\ 0 & 2 & 4 \\ 1 & 4 & 3 \end{pmatrix};$$

where $v_d = h v_d i$ is the VEV of the Higgs field. In M_d , the i 's are $O(1)$ (complex) coefficients, given in terms of the i 's. Ref. [3] shows that such a pattern of the mass matrix explains the quark masses and CKM elements.

If $U(2)$ is still a good symmetry at the SUSY breaking scale, and broken (spontaneously) only below the SUSY breaking scale, the SUSY breaking terms would have a structure dictated by $U(2)$. For our purposes it is sufficient to consider the down sector squark mass matrices, and they are given as

$$L \quad (\tilde{q}_L \quad \tilde{s}_L \quad \tilde{b}_L) M_{LL}^2 (\tilde{q}_L \quad \tilde{s}_L \quad \tilde{b}_L) + (\tilde{q}_R \quad \tilde{s}_R \quad \tilde{b}_R) M_{RR}^2 (\tilde{q}_R \quad \tilde{s}_R \quad \tilde{b}_R) + (\tilde{q}_R \quad \tilde{s}_R \quad \tilde{b}_R) M_{RL}^2 (\tilde{q}_L \quad \tilde{s}_L \quad \tilde{b}_L) + h.c. ; \quad (4)$$

$$M_{LL}^2 = M_d^y M_d + \begin{pmatrix} 0 & m_1^2 & i^0 m_5^2 & 0 & 1 \\ i^0 m_5^2 & m_1^2 + m_2^2 & m_4^2 & 0 & 0 \\ 0 & m_1^2 & i^0 m_5^2 & m_3^2 & 1 \\ 0 & i^0 m_5^2 & m_1^2 + m_2^2 & m_4^2 & 0 \\ 0 & 0 & 0 & m_3^2 & 1 \end{pmatrix}_{LL} + D \text{ term} ;$$

$$M_{RR}^2 = M_d^y M_d + \begin{pmatrix} 0 & m_4^2 & m_3^2 & 0 & 1 \\ m_4^2 & m_1^2 & i^0 m_5^2 & 0 & 0 \\ 0 & i^0 m_5^2 & m_1^2 + m_2^2 & m_4^2 & 0 \\ 0 & 0 & 0 & m_3^2 & 1 \end{pmatrix}_{RR} + D \text{ term} ;$$

$$M_{RL}^2 = \tan M_d + v_d \begin{pmatrix} 0 & A_1 & 0 & A_2 & A_4 \\ 0 & A_1 & 0 & A_2 & A_4 \\ 0 & 0 & A_1 & 0 & A_3 \end{pmatrix}; \quad (5)$$

where m_i^2 and A_i are determined by the SUSY breaking mechanism. Here m_1^2, m_2^2, m_3^2 and m_5^2 are real, while m_4^2 and A_i could be complex. We will assume that the A_i are of order A , a common mass scale. The D terms are flavor diagonal, and since we are interested in FCNC processes, we will not write them in detail, but will think of them as included in m_1^2 and m_3^2 .

Thus far we have presented the mass matrices in the gauge basis. In the following sections, we will work in the superKM basis in which the quark mass matrix is diagonal, and the quark field rotations that diagonalize the quark mass matrix are applied to the squarks, whose mass matrix would also have been diagonalized in the MFV scheme. Since we will not assume an MFV structure, in the superKM basis, there would be small diagonal terms in the squark mass matrix, which we treat as perturbations. The structure of the squark mass matrix in the superKM basis is similar to that in Eq. (5) owing to the smallness of the mixing angles that diagonalize the quark mass matrix.

B. SUSY parameters

Lacking specific knowledge about the SUSY breaking mechanism realized in nature, we make some assumptions on the SUSY mass spectrum. Neutron EDM places strong constraints on the CP violating phases and the masses of the first two generations of scalars. To satisfy this and other collider constraints, we consider an "effective SUSY" framework in which the scalars of the first two generations are heavy, suppressing EDM, and allowing for larger CP violating phases. Defining the scalar mass scale, $m_0 = 1 \text{ TeV}$, we take all $m_i = m_0$ except for $m_{\tilde{t}_R, \tilde{b}_R} = 100 \text{ GeV}$. We take $A = m_0$, the gaugino mass parameter M_2 and charged-Higgs masses to be 250 GeV and the gluino mass to be 300 GeV². We summarize our choice of the parameters in Table I. We assume such a spectrum just above the weak scale without specifying what mechanism of SUSY breaking and mediation might actually give rise to it. As we will show later, if realized in nature such a spectrum would lead to enhancements in the processes we are considering here. We will also show that the values in Table I are compatible with present experimental data and will vary these parameters around the values chosen to show its effect on various quantities.

The rates of various FCNC processes follow from the mass matrix that we have specified in Eq. (5). We will work in the superKM basis. We note that stop and sbottom mixing in

² The Tevatron bounds on the stop, sbottom and gluino masses are discussed in Ref. [9]. We note here that the bounds in general get less stringent as the neutralino mass increases.

our case are negligibly small, c.f. Appendix A. The interaction vertices in the mass basis are obtained by diagonalizing the mass matrices in Eq. (5), and the perturbative diagonalization to leading order is shown in Appendix A.

The dominant NM FV contribution from SUSY would be due to the 32 and 23 entries in Eq. (5), since it is the biggest off-diagonal term. For convenience we define

$$\frac{M_{R\bar{L},R\bar{R},L\bar{L}}^2}{m_0^2} d_{32,23} : \quad (6)$$

Since we have written down an effective theory and not specified the dynamics of U(2) and

m_0	1000	$\tan\theta$	5
$m_{\tilde{b}_R, \tilde{b}_R}$	100		$200 e^{i2:2}$
$m_{\tilde{d}_R, \tilde{d}_R}$	1000	M_2	250
$m_{\tilde{q}_L}$	1000	M_g	300
A	1000	m_H	250
$d_{32}^{R\bar{L}}$	$2 e^{i3:2}$	$d_{32}^{R\bar{R}}$	$1:75 e^{i1:6}$

TABLE I: Default SUSY parameters for this work that satisfies all experimental constraints discussed in this paper. All masses are in GeV.

SUSY breaking, we can only specify the order of magnitude of $d_{32,23}$, and for the parameters shown in Table I, it is

$$d_{32,23}^{R\bar{L}} = \frac{v_d A}{m_0^2} d_{32,23}^{R\bar{L}} = 6.82 \cdot 10^{-4} d_{32,23}^{R\bar{L}} ; \quad d_{32,23}^{R\bar{R}} = \frac{m_4^2}{m_0^2} d_{32,23}^{R\bar{R}} = 0.02 d_{32,23}^{R\bar{R}} : \quad (7)$$

This specifies the natural size of d_{32} , and when we describe FCNC effects, we will illustrate the range of possible values by varying its (O(1)) unknown coefficient, d_{32} .

We will find that $d_{32}^{R\bar{L}}$ induces NM FV $B = 1$ FCNC processes dominantly, while $d_{32,23}^{R\bar{R},L\bar{L}}$ induces $S = 2$ and $B = 2$ FCNC processes. Though the $d_{32}^{R\bar{L}}$ and $d_{23}^{R\bar{L}}$ elements have similar magnitudes, the $d_{32}^{R\bar{L}}$ gluino NM FV contribution to $B = 1$ FCNC processes is larger, since we take \tilde{b}_R to be much lighter than the other scalars, and the $d_{23}^{R\bar{L}}$ gluino diagrams are relatively suppressed by the heavier \tilde{b}_L mass. Therefore, in this work we will include only the dominant $d_{32}^{R\bar{L}}$ contribution. We illustrate this in Fig. 1, where we show the

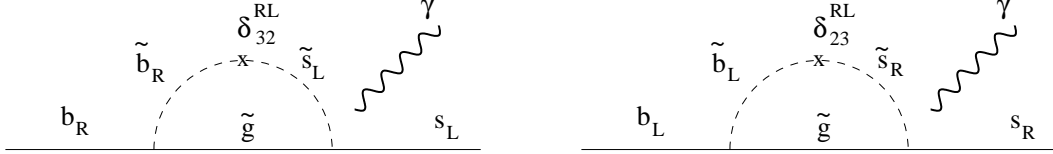


FIG. 1: Gluino contribution to $B_d \rightarrow X_s$. The diagram on the left, proportional to δ_{32}^{RL} , has the lighter scalar \tilde{b}_R , while the one on the right, proportional to δ_{23}^{RL} , only has heavier scalars and is therefore relatively suppressed.

gluino contribution to $B_d \rightarrow X_s$ as an example. Similarly, owing to the smaller \tilde{b}_R mass, the $\delta_{32;23}^{RR}$ NM FV contribution to $S = 2$ and $B = 2$ FCNC processes is relatively larger compared to the $\delta_{32;23}^{LL}$ contribution.

In the next three sections we will discuss the implication of the U(2) model to $S = 2$, $B = 2$ and $B = 1$ FCNC processes. From this we will see that present experimental data are compatible with the values shown in Table I, and we will obtain expectations for some measurements that are forthcoming.

III. $S = 2$ FCNC PROCESS

The CP violation parameter j_K due to mixing in the K meson sector has been measured to be [10]

$$j_K = (2.284 \pm 0.014) \times 10^3 : \quad (8)$$

We wish to estimate the new physics contributions to j_K in the scenario that we are considering. Here we note that even though the direct CP violation parameter $j_K^0 = j_K$ has also been measured, large hadronic uncertainties do not permit us to constrain new physics models through this observable.

K meson mixing is governed by the $S = 2$ effective Hamiltonian

$$H_{S=2}^{\text{eff}} = C_1 Q_1 \quad (9)$$

with the operator $Q_1 = d_L \bar{s}_L d_L \bar{s}_L$, where we show only the operator Q_1 since in the SM

and the new physics model we are considering, the dominant contributions are only to this operator. The CP violation parameter ϵ_K is then given by (see for example Ref. [12])

$$\epsilon_K = e^{i\pi/4} \frac{1}{3} \frac{m_K B_K f_K^2}{2 m_K} \text{Im} [C_1(m_K)] ; \quad (10)$$

where B_K is the Bag parameter and f_K is the Kaon decay constant.

In addition to the SM W box diagram contribution to C_1 , in the supersymmetric $U(2)$ theory we are considering, the charged-Higgs and chargino MFV contributions could be sizable. The dominant MFV contributions to C_1 can be written as

$$C_1^{\text{MFV}} = C_1^W + C_1^H + C_1 ; \quad (11)$$

which is the sum of the SM W , the charged-Higgs, and the chargino contributions, respectively.

SM contribution: The SM W contribution is [11]

$$C_1^{\text{SM}}(m_t) = C_1^W(m_t) = \frac{G_F^2 m_W^2}{4^2} \left((V_{td} V_{ts})^2 S_0(x_t) + (V_{cd} V_{cs})^2 S_0(x_c) + 2 (V_{td} V_{ts} V_{cd} V_{cs}) S_0(x_t; x_c) \right) ; \quad (12)$$

where the function S_0 is given in Appendix B, Eq. (B3), and $x_t = m_t^2/m_W^2$, $x_c = m_c^2/m_W^2$.

The QCD correction due to renormalization group running from m_t to m_b gives

$$C_1^{\text{SM}}(m_K) = C_1^W(m_K) = \frac{G_F^2 m_W^2}{4^2} \left((V_{td} V_{ts})^2 \kappa_{33} S_0(x_t) + (V_{cd} V_{cs})^2 \kappa_{22} S_0(x_c) + 2 (V_{td} V_{ts} V_{cd} V_{cs}) \kappa_{32} S_0(x_t; x_c) \right) ; \quad (13)$$

where the κ_K are QCD correction factors given in Eq. (18) below, and V_{ij} are the CKM matrix elements.

Charged-Higgs contribution: Supersymmetric theories require two Higgs doublets to give masses to the up and down type fermions. The Higgs doublets contain the charged-Higgs H^\pm , and the dominant charged-Higgs-top contribution is [12]

$$C_1^H(m_t) = \frac{G_F^2 m_W^2}{4^2} (V_{td} V_{ts})^2 \kappa^H \frac{F_V^H}{2} ; \quad (14)$$

$$F_V^H = \frac{1}{4 \tan^4} x_t^2 Y_1(r_H; r_H; x_t; x_t) + \frac{1}{2 \tan^2} x_t^2 Y_1(1; r_H; x_t; x_t) - \frac{2}{\tan^2} x_t Y_2(1; r_H; x_t; x_t) ;$$

where $r_H = m_H^2/m_W^2$, and the functions Y_1 and Y_2 are given in Appendix B, Eq. (B 4).

Chargino contribution: The dominant chargino-right-handed-stop contribution is [12]

$$C_1(m_t) = \frac{G_F^2 m_W^2}{4^2} (V_{td} V_{ts})^2 [F_V];$$

$$F_V = \frac{1}{4} j_R^{(i)} \bar{j}_R^{(j)} j_R^{(j)} \bar{j}_R^{(i)} Y_1(r_{t_2}; r_{t_2}; s_i; s_j);$$
(15)

where $r_{t_2} = m_{t_2}^2/m_W^2$, $s_{1,2} = m_{\tilde{t}_{1,2}}^2/m_W^2$, and the coupling is given by

$$j_R^{(i)} = \frac{(C_R)_{2i}}{\sin \theta_W} \frac{m_t}{m_W};$$
(16)

with the diagonalization matrix (C_R) given in Appendix A, Eq. (A 6). Taking into account renormalization group running, we have

$$C_1^H; (m_K) \quad \kappa_{33} C_1^H; (m_t);$$
(17)

Glino contribution: The NMHV glino contributions is not significant due to a suppression from the heavy \tilde{d} and \tilde{s} masses, \tilde{W} suppression owing to their approximate degeneracy (split only by $O(\epsilon^2)$, c.f. Eq. (5)), and the contribution from the relatively light right-handed sbottom being suppressed by its small mixing to the first two generations. Moreover, owing to the structure of the mass matrix, Eq. (5), the glino contribution is real, and hence does not contribute to κ .

In our numerical analysis, we take the following values for the various parameters [10, 11]:

$$\kappa_{33} = 0.57; \quad \kappa_{22} = 1.38; \quad \kappa_{32} = 0.47;$$

$$f_K = 0.160 \text{ GeV}; \quad 0.6 < B_K < 0.9;$$

$$m_K = 0.497 \text{ GeV}; \quad m_K = (3.48 \quad 0.01) \quad 10^{15} \text{ GeV}; \quad m_c = (1.2 \quad 0.2) \text{ GeV};$$
(18)

The SM prediction for κ is in agreement with the experimental data, but it should be noted that there is considerable uncertainty in the lattice computation of the Bag parameter B_K (see Eq. (18)). The chargino and charged-Higgs contributions to C_1 add constructively with the SM contribution. Therefore, if the true value of B_K is taken to be closer to the lower limit, we can allow MFV contributions to be up by a factor of 1.2 compared to the SM value; i.e., $\text{Im}(C_1^{\text{MFV}}) = \text{Im}(C_1^{\text{SM}}) < 1.2$. Fig. 2 shows the region of MFV parameter space

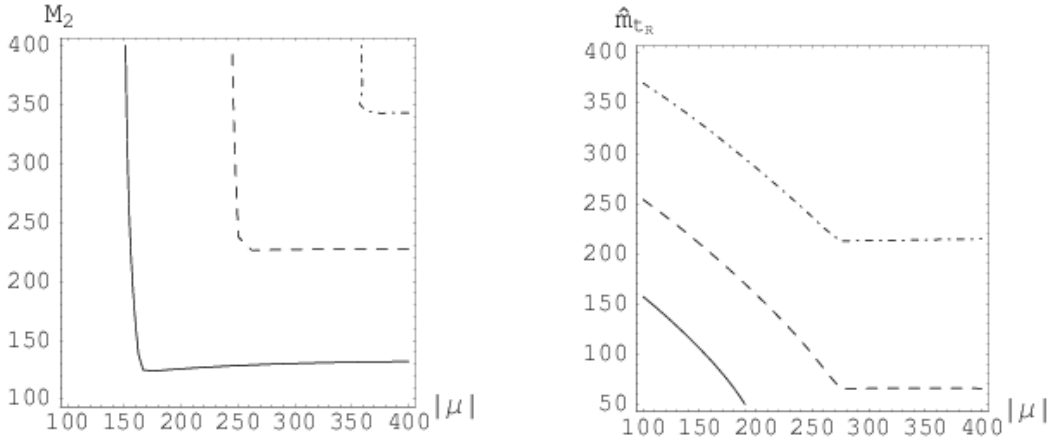


FIG. 2: The (dash-dot, dash, solid) curves are (1.05, 1.1, 1.2) contours of $\text{Im}(C_1^{\text{MFV}}) = \text{Im}(C_1^{\text{SM}})$, showing the M FV contributions to K aon mixing relative to the SM .

where this is satisfied. This justifies some of the choices we make in the list shown in Table I.

IV. $B = 2$ FCNC PROCESSES

A. General formalism

We start by discussing in general $B_q B_q$ mixing and later specialize in succession to $B_d B_d$ ($q=d$) and to $B_s B_s$ ($q=s$). The $B=2$ effective Hamiltonian is given by [13]:

$$H_{B=2}^{\text{eff}} = \sum_{i=1}^{x^5} C_i Q_i + \sum_{i=1}^{x^3} C_i \tilde{Q}_i ; \quad (19)$$

where, for B_q ,

$$Q_1 = q_L b_L q_L b_L ;$$

$$Q_2 = q_R b_L q_R b_L ;$$

$$Q_3 = q_R b_L q_R b_L ;$$

$$Q_4 = q_R b_L q_L b_R ;$$

$$Q_5 = q_R b_L q_L b_R : \quad (20)$$

The operators Q_i ($i=1,2,3$) are obtained by exchanging $L \leftrightarrow R$. The Wilson coefficients C_i are run down from the SUSY scale, M_S , using [13]

$$C_r(m_b) = \sum_{i=s}^{X-X} b_i^{(r;s)} + G_i^{(r;s)} a_i C_s(M_S) \quad (21)$$

where $s(M_S) = s(m_t)$ and the a_i, b_i and c_i are constants given in Ref. [13].

The matrix elements of the Q_i in the vacuum insertion approximation are given by [13, 15].

$$\begin{aligned} B_q^D \mathcal{D}_1(B_q) \mathcal{B}_q^E &= \frac{2}{3} m_{B_q}^2 f_{B_q}^2 B_1(); \\ B_q^D \mathcal{D}_2(B_q) \mathcal{B}_q^E &= \frac{5}{12} \frac{m_{B_q}}{m_b + m_q} m_{B_q}^2 f_{B_q}^2 B_2(); \\ B_q^D \mathcal{D}_3(B_q) \mathcal{B}_q^E &= \frac{1}{12} \frac{m_{B_q}}{m_b + m_q} m_{B_q}^2 f_{B_q}^2 B_3(); \\ B_q^D \mathcal{D}_4(B_q) \mathcal{B}_q^E &= \frac{1}{2} \frac{m_{B_q}}{m_b + m_q} m_{B_q}^2 f_{B_q}^2 B_4(); \\ B_q^D \mathcal{D}_5(B_q) \mathcal{B}_q^E &= \frac{1}{6} \frac{m_{B_q}}{m_b + m_q} m_{B_q}^2 f_{B_q}^2 B_5(); \end{aligned} \quad (22)$$

where we take for the decay constants $f_{B_q} = 0.2 - 0.03$ GeV and the for the Bag parameters (at scale m_b) $B_1 = 0.87, B_2 = 0.82, B_3 = 1.02, B_4 = 1.16$ and $B_5 = 1.91$ [13, 15].

The B_q mass difference is given by

$$m_{B_q} = 2 M_{12}(B_q) j; \quad (23)$$

where $M_{12}(B_q)$ is the off-diagonal Hamiltonian element for the $B_q B_q$ system, and is given by

$$M_{12} = M_{12}^{SM} + M_{12}^{SUSY};$$

$$_{12}^{SM} : \quad$$

M_{12} to an excellent approximation is dominated by the SM tree decay modes. From Refs. [14, 15] we have,

$$M_{12}(B_q) j = \frac{1}{2m_{B_q}} B_q^D \mathcal{H}_{B=2}^{\text{eff}} \mathcal{B}_q^E; \quad$$

$$\begin{aligned}
{}_{12}^{\text{SM}} = & (-1) \frac{G_F^2 m_b^2 m_{B_q} B_{B_q} f_{B_q}^2}{8} v_t^2 + \frac{8}{3} v_c v_t (z_c + \frac{1}{4} z_c^2 - \frac{1}{2} z_c^3) \\
& + v_c^2 \frac{p}{1 - 4z_c} (1 - \frac{2}{3} z_c) + \frac{8}{3} z_c + \frac{2}{3} z_c^2 - \frac{4}{3} z_c^3 \quad 1 \quad ;
\end{aligned} \quad (24)$$

where $v_x = V_{xb} V_{xq}$, $z_c = \frac{m_c^2}{m_b^2}$ and we take $B_{B_q} = 1.37$.

The dilepton asymmetry in B_q is given by [16]

$$A_{11}^{B_q} = \frac{N(B_q B_q)}{N(B_q B_q) + N(B_q B_q)} = \text{Im} \frac{12}{M_{12}} \quad ; \quad (25)$$

We discuss next the SM and new physics contributions to the coefficients C_i and C'_i .

M FV contribution: The SM W contribution is almost identical to that shown in Eq.(12) but for the fact that it is sufficient to keep only the top contribution (the $S_0(x_t)$ term) and changing the CKM factor to $V_{tq} V_{tb}^2$. The new physics M FV charged-Higgs and chargino contributions are again identical to Eqs. (14) and (15), respectively, with the same change for the CKM factors. $C_1(m_t)$ is evolved down to m_b using Eq. (21).

Gluino contribution: We only include the dominant gluino-right-handed-bottom box diagrams with ${}_{32}^{\text{RL}}$ and ${}_{32}^{\text{RR}}$ mass insertions, since b_R is the only relatively light down type squark in our scenario. These contributions are given by [6]

$$\begin{aligned}
C_1^g(M_g) &= i g_s^4 {}_{b3}^{\text{RR}} {}_{q3}^{\text{RR}} {}_{i_2}^{\text{h}} \frac{1}{36} I_4 + \frac{1}{9} M_g^2 I_4 \quad ; \\
C_2^g(M_g) &= i g_s^4 {}_{b3}^{\text{RL}} {}_{q3}^{\text{RL}} {}_{i_2}^{\text{h}} \frac{3}{2} M_g^2 I_4 \quad ; \\
C_3^g(M_g) &= i g_s^4 {}_{b3}^{\text{RL}} {}_{q3}^{\text{RL}} {}_{i_2}^{\text{h}} \frac{1}{2} M_g^2 I_4 \quad ;
\end{aligned} \quad (26)$$

with the box integrals I_4 and I_4' given in Appendix B. The couplings are given by

$$\begin{aligned}
{}_{b3}^{\text{RR}} &= \cos {}_{32}^{\text{RR}} \quad ; \quad {}_{b3}^{\text{RL}} = \cos {}_{32}^{\text{RL}} \quad ; \\
{}_{d3}^{\text{RR}} &= \sin {}_{12}^{\text{RR}} \sin {}_{32}^{\text{RR}} e^{i(\frac{RR}{32} + \frac{RR}{12})} \quad ; \quad {}_{s3}^{\text{RR}} = \cos {}_{12}^{\text{RR}} \sin {}_{32}^{\text{RR}} e^{i \frac{RR}{32}} \quad ; \\
{}_{d3}^{\text{RL}} &= \sin {}_{12}^{\text{RL}} \sin {}_{32}^{\text{RL}} e^{i(\frac{RL}{32} + \frac{RL}{12})} \quad ; \quad {}_{s3}^{\text{RL}} = \cos {}_{12}^{\text{RL}} \sin {}_{32}^{\text{RL}} e^{i \frac{RL}{32}} \quad ;
\end{aligned} \quad (27)$$

obtained from the 3 3 mixing matrix that is the product of $C_{d_R s_R}$ and $C_{b_R s_R}$, with the mixing angles and phases given in Appendix A. In our U(2) model, if m_4 is of the same

order as A , based on the estimate in Eq. (7), we expect C_1^g to receive the dominant gluino contribution from $\tilde{\alpha}_R \tilde{s}_R$. We will focus on this contribution in the following.

We point out in Appendix A, Eq. (A18), that $\tilde{\alpha}_R \tilde{s}_R$ mixing can be generically large (near maximal), in which case the gluino contributions to both $B_d B_d$ and $B_s B_s$ mixing can be sizable. However, if $m_5^2 \ll m_2^2$, this mixing can be small and the gluino contribution to $B_d B_d$ mixing is negligible since it is proportional to $\sin \frac{\pi}{12}$, c.f. Eqs. (26) and (27). The gluino contribution to $B_s B_s$, however, can still be sizable in either case since it is proportional to $\cos \frac{\pi}{12}$.

B. $B_d B_d$ mixing

The $B_d B_d$ mass difference (m_d), and CP violation in $B_d \rightarrow K_s (\bar{a}_{K_s})$ have been measured to be [10, 17],

$$\begin{aligned} m_d &= 0.502 \pm 0.007 \text{ ps}^{-1}; \\ a_{K_s} &= 0.725 \pm 0.037; \end{aligned} \quad (28)$$

In the SM, the usual notation is, $a_{K_s}^{SM} = \sin 2\beta$.

As we have already pointed out in Section III, the charged-Higgs and chargino MFV contributions add constructively with the SM contribution. The SM prediction agrees quite well with the data, but given the uncertainty in f_{B_d} , c.f. below Eq. (22), it might be possible to accommodate an MFV contribution up to a factor of about 1.3 bigger than the SM contribution. We show in Fig. 3 the region in MFV parameter space that satisfies this constraint, ignoring the gluino contribution.

As pointed out in the previous subsection, in general we expect in the $U(2)$ model, $\tilde{\alpha}_R \tilde{s}_R$ mixing to be near maximal, in which case the gluino contribution to $B_d B_d$ can be sizable. The gluino contribution can then be important to both m_d and a_{K_s} . Taking this into account, we can write $a_{K_s} = \sin(2\beta + 2\delta)$, where δ is the new phase in $M_{12}(B_d)$ [18], and

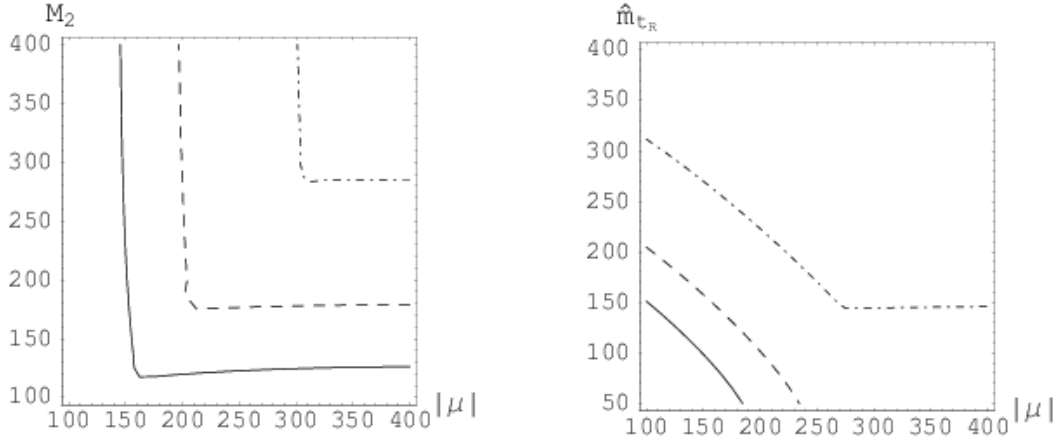


FIG . 3: The (dash-dot, dash, solid) curves are (1.1, 1.2, 1.3) contours of $\mathcal{C}_1^{\text{MFV}} = \mathcal{C}_1^{\text{SM}}$; showing the M FV contributions to $B_d B_d$ mixing relative to the SM .

we have [10, 19]

$$\begin{aligned} a_{K_s} &= \text{Im} (\bar{K}) ; \\ \bar{K} &= \frac{q A (B_d ! - K_s)}{p A (B_d ! - K_s)} ; \quad \frac{q}{p} \frac{\bar{u}}{\bar{t}} \frac{M_{12} - \frac{i}{2} \gamma_{12}}{M_{12} + \frac{i}{2} \gamma_{12}} ; \end{aligned} \quad (29)$$

with M_{12} and γ_{12} given in Eq. (24). (The " sign in \bar{K} is because the final state is CP odd.) In our case, $\gamma_{12} = M_{12}$, so that

$$a_{K_s} = \sin(\arg(M_{12})) ; \quad (30)$$

where "arg" denotes the argument of the complex quantity.

For the case when $\tilde{d}_R s_R$ mixing is large, we show the gluino contribution to $B_d B_d$ in Fig 4. The plot on the left also shows the constraint from a_{K_s} , which is not shown in the plot on the right since almost the whole region shown is allowed. The region ($0 < \arg(\frac{R_R}{32}) < 2\pi$) is not shown since it is identical to the region $(0; \pi)$. From the figure, we see that in the large mixing case, the constraint on $\frac{R_R}{32}$ is quite strong. However, if $\tilde{d}_R s_R$ mixing is small, the constraint on $\frac{R_R}{32}$ from $B_d B_d$ mixing is weak.

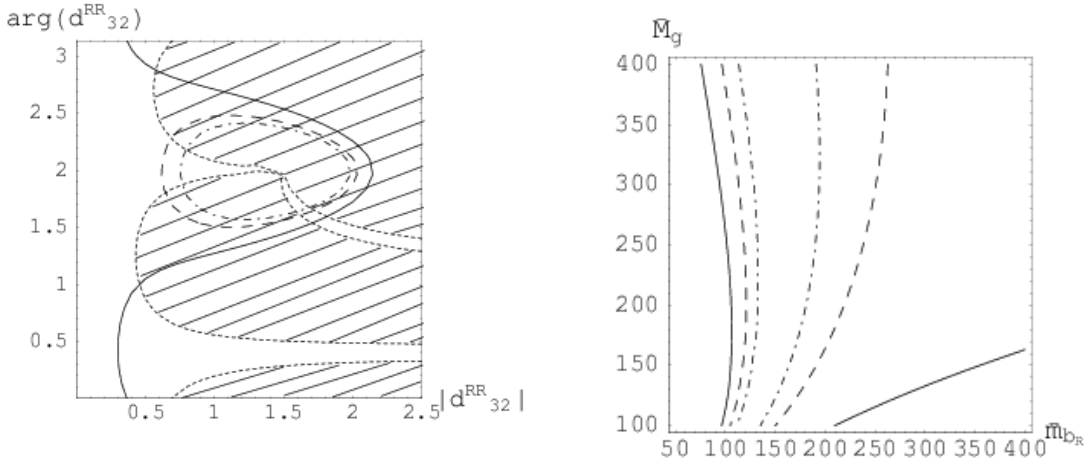


FIG . 4: For large $\tilde{d}_R s_R$ mixing, the (dash-dot, dash, solid) curves are (0.9, 1.0, 1.25) contours of $j(C_1 + C_1^*) = C_1^{\text{SM}}/j$ showing the NM FV contributions to $B_d B_d$ mixing relative to the SM . d_{32}^{RR} is defined in Eq. (7). The hatched region is excluded by a χ_s .

C . $B_s B_s$ mixing

$B_s B_s$ mixing has not yet been observed and the current experimental limit is $m_{B_s} > 14.4 \text{ ps}^{-1}$ at 95% C.L. [10]. The SM prediction is: $14 \text{ ps}^{-1} < m_{B_s} < 20 \text{ ps}^{-1}$ [20]. The SM prediction for the dilepton asymmetry $A_{11}^{B_s}$ is small, around 10^{-4} , c.f. references in Ref.[16].

$B_s B_s$ mixing depends quite sensitively on d_{32}^{RR} , and for the region in Fig. 4 allowed by $B_d B_d$ mixing, we find $m_{B_s} = 22 \text{ ps}^{-1}$ and $A_{11}^{B_s} = 5 \cdot 10^{-4}$. This m_{B_s} is a little higher than the SM prediction, although may be within the SM allowed range, given uncertainties.

As we pointed out in the previous subsection, if $\tilde{d}_R s_R$ mixing is small, then the $B_d B_d$ mixing constraints on d_{32}^{RR} becomes weak. If such is the case, there are essentially no constraints from $B_d B_d$ mixing, and we show contours of m_{B_s} and $A_{11}^{B_s}$ in Fig. 5. We show only the range $(0 < \arg(d_{32}^{RR}) < \pi)$, since the $(-\pi/2, \pi/2)$ range is identical to this. It can be seen that m_{B_s} can increase significantly above the SM prediction. The projected Run II sensitivity for m_{B_s} at the Tevatron with 2 fb^{-1} is around 40 ps^{-1} [20], and can probe

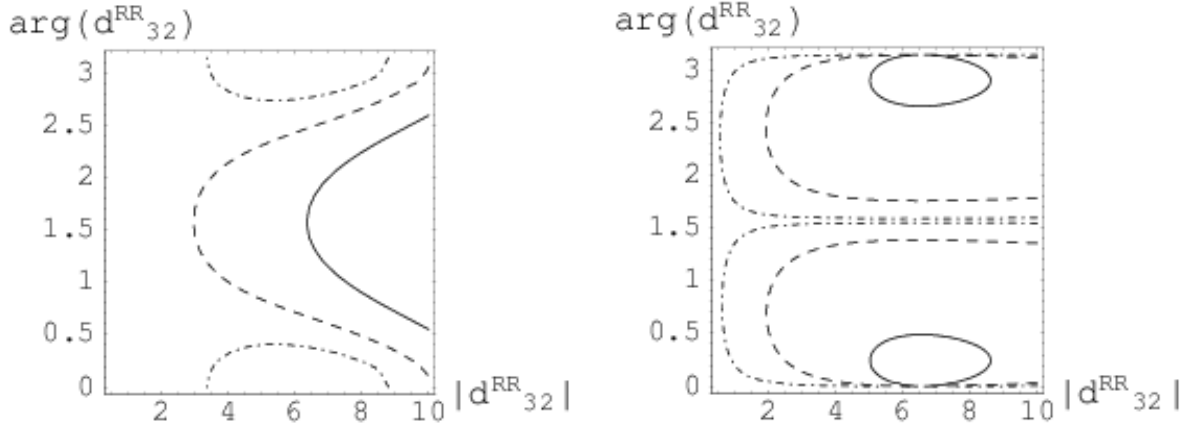


FIG. 5: For small d_R s_R fixing, the (dash-dot, dash, solid) curves are $(15, 25, 40 \text{ ps}^{-1})$ contours of m_{B_s} (left), and $(10^{-4}, 10^{-3} \text{ and } 10^{-2})$ contours of $A_{11}^{B_s}$ (right). d_{32}^{RR} is defined in Eq. (7).

a significant region of $U(2)$ parameter space. If a higher value of m_{B_s} is measured than what the SM predicts, it would indicate the presence of new physics. Measuring $A_{11}^{B_s}$ can also significantly constrain d_{32}^{RR} as can be seen from Fig. 5 (right).

V. $B = 1$ F C N C P R O C E S S E S

A. Effective Hamiltonian

The $B = 1$ effective Hamiltonian at a scale Λ in the operator product expansion (OPE) is [11, 21, 22]

$$H_{B=1}^{\text{eff}} = \frac{G_F}{2} V_{ts} V_{tb} \sum_{i=1,6,9,10}^X C_i(\Lambda) O_i(\Lambda) + C_7(\Lambda) O_7(\Lambda) + C_{8g}(\Lambda) O_{8g}(\Lambda)^A; \quad (31)$$

with

$$O_1 = (s \bar{c})_{VA} (c \bar{b})_{VA};$$

$$\begin{aligned}
O_2 &= (sc)_V \underset{A}{\underset{X}{\underset{q}{\underset{q}{(sb)}}}} (db)_V \underset{A}{\underset{X}{\underset{q}{\underset{q}{(qq)}}}}; \\
O_3 &= (sb)_V \underset{A}{\underset{X}{\underset{q}{\underset{q}{(q q)}}}} (q q)_V \underset{A}{\underset{X}{\underset{q}{\underset{q}{(q q)}}}}; \\
O_4 &= (s b)_V \underset{A}{\underset{X}{\underset{q}{\underset{q}{(q q)}}}} (q q)_V \underset{A}{\underset{X}{\underset{q}{\underset{q}{(q q)}}}}; \\
O_5 &= (sb)_V \underset{A}{\underset{X}{\underset{q}{\underset{q}{(q q)}}}} (q q)_{V+A}; \\
O_6 &= (s b)_V \underset{A}{\underset{X}{\underset{q}{\underset{q}{(q q)}}}} (q q)_{V+A}; \\
O_7 &= \frac{e}{8^2} m_b s (1 + \gamma_5) b F; \\
O_{8g} &= \frac{g_s}{8^2} m_b s (1 + \gamma_5) T^a b G^a; \\
O_9 &= (sb)_V \underset{A}{\underset{X}{\underset{q}{\underset{q}{(ee)}}}} (ee)_V; \\
O_{10} &= (sb)_V \underset{A}{\underset{X}{\underset{q}{\underset{q}{(ee)}}}} (ee)_A; \tag{32}
\end{aligned}$$

where, the subscript (V A) means $(1 \gamma_5)$, and F, G are the electromagnetic and color field strengths, respectively.

The Wilson coefficients can be computed at the scale M_W (the W boson mass), and then run down to the scale m_b (the b quark mass). Below, when no scale is specified for the coefficients, it is understood to be at m_b , i.e., $C_i = C_i(m_b)$. The coefficients when run down from M_W to m_b mix under renormalization, so that [23]

$$\begin{aligned}
C_j &= \sum_{i=1}^{X^8} k_{ji}^{a_i}; \quad (j = 1, \dots, 6); \\
C_7 &= \frac{16}{32} C_7(M_W) + \frac{8}{3} \frac{14}{32} C_{8g}(M_W) + \sum_{i=1}^{X^8} h_i^{a_i} C_2(M_W); \\
C_{8g} &= \frac{14}{32} C_{8g}(M_W) + \sum_{i=1}^{X^8} h_i^{a_i} C_2(M_W); \tag{33}
\end{aligned}$$

where $\frac{s(M_W)}{s(m_b)} = 0.56$ and h_i, h_i, a_i and k_{ji} are given in Ref. [11]. In addition, the evolution equation for C_9 is given in Ref. [22], and C_{10} is not renormalized.

Separating out the new physics contribution to the renormalization group evolution, i.e., Eq. (33), we get

$$\begin{aligned}
C_2 &= C_2^{\text{SM}}; \\
C_7 &= C_7^{\text{SM}} + 0.67 C_7^{\text{new}}(M_W) + 0.09 C_{8g}^{\text{new}}(M_W);
\end{aligned}$$

$$C_{8g} = C_{8g}^{SM} + 0.70 C_{8g}^{new}(M_W); \quad (34)$$

in which the superscript "SM" indicates the contribution from the SM, and "new" from new physics.

SM contribution: The SM W contribution to $C_7(M_W)$ and $C_{8g}(M_W)$ are given by [24, 25]

$$C_2^{SM}(M_W) = 1; \quad (35)$$

$$C_{7,8g}^{SM}(M_W) = \frac{3}{2} F_{7,8}^{LL} \frac{m_t^2}{M_W^2}; \quad (36)$$

where $F_{7,8}^{LL}(x)$ are given in Appendix B. Using Eq. (33) we can compute C_2^{SM} , C_7^{SM} and C_{8g}^{SM} .

In the following, we will discuss, in order, the new physics contribution arising from the charged-Higgs boson (H), charginos ($\tilde{\chi}$) and gluinos (\tilde{g}).

Charged Higgs (H) contribution: The charged-Higgs contribution to $B_d \rightarrow X_s$ is given by [5, 25, 26]

$$C_{7,8g}^H(M_W) = \frac{1}{2} \cot^2 \theta_W F_{7,8}^{LL} \frac{m_t^2}{M_H^2} + F_{7,8}^{LL} \frac{m_t^2}{M_H^2}; \quad (37)$$

where $F_{7,8}^{LL}(x)$ and $F_{7,8}^{RL}(x)$ are given in Appendix B.

Chargino ($\tilde{\chi}$) contribution: The chargino-stop contribution can be comparable to the SM contribution for a light stop and chargino. In the scenario that we are considering, the stop mixing angle is negligibly small and $m_{\tilde{t}_1} \approx m_0$ and $m_{\tilde{t}_2} \approx M_W$. We therefore run the \tilde{t}_1 contribution from m_0 down to M_W and evaluate the \tilde{t}_2 contribution at M_W . The chargino-stop contribution is [5, 25, 26]

$$C_{7,8g}^{\tilde{t}_1}(m_0) = \sum_{j=1}^{x^2} \left[\frac{1}{L} \frac{1}{j} \frac{M_W^2}{m_{\tilde{t}_1}^2} F_{7,8}^{LL} \frac{m_{\tilde{t}_1}^2}{M_{\tilde{\chi}_j}^2} + \frac{1}{R} \frac{1}{j} \frac{M_W}{m_{\tilde{t}_1}} F_{7,8}^{RL} \frac{m_{\tilde{t}_1}^2}{M_{\tilde{\chi}_j}^2} \right];$$

$$C_{7,8g}^{\tilde{t}_2}(M_W) = \sum_{j=1}^{x^2} \left[\frac{2}{L} \frac{2}{j} \frac{M_W^2}{m_{\tilde{t}_2}^2} F_{7,8}^{LL} \frac{m_{\tilde{t}_2}^2}{M_{\tilde{\chi}_j}^2} + \frac{2}{R} \frac{2}{j} \frac{M_W}{m_{\tilde{t}_2}} F_{7,8}^{RL} \frac{m_{\tilde{t}_2}^2}{M_{\tilde{\chi}_j}^2} \right]; \quad (38)$$

where the loop functions $F_{7,8}^{RL}$ are given in Appendix B, and $\frac{ij}{L}$ and $\frac{ij}{R}$ contain the stop and chargino mixing matrices. Explicit expressions for $\frac{ij}{L}$, $\frac{ij}{R}$ and the renormalization group

equations to evolve $C_{7,8g}^{\tilde{t}_1}(m_0)$ down to M_W are given in Ref. [25].

Glino (g) contribution: In our NM FV scenario, the gluino contributions can be sizable since they couple with strong interaction strength. Furthermore, because the sbottom mixing angle is negligibly small, $m_{\tilde{b}_1} \approx m_0$ and $m_{\tilde{b}_2} \approx M_W$. Keeping only the $\frac{M_g}{m_b}$ enhanced piece, the gluino contribution is [5]

$$C_{7g}^g(M_W) = \frac{4}{G_F} \frac{s}{2} \frac{M_g}{m_b} \cos \frac{R_L}{32} \sin \frac{R_L}{32} e^{i \frac{R_L}{32}} \frac{1}{9} \frac{1}{m_{\tilde{b}_2}^2} F_4 @ \frac{M_g^2}{m_{\tilde{b}_1}^2} A \frac{1}{m_{\tilde{b}_1}^2} F_4 @ \frac{M_g^2}{m_{\tilde{b}_1}^2} A \frac{5}{3};$$

$$C_{8g}^g(M_W) = \frac{4}{G_F} \frac{s}{2} \frac{M_g}{m_b} \cos \frac{R_L}{32} \sin \frac{R_L}{32} e^{i \frac{R_L}{32}} \frac{1}{8} \frac{1}{m_{\tilde{b}_2}^2} F_g @ \frac{M_g^2}{m_{\tilde{b}_1}^2} A \frac{1}{m_{\tilde{b}_1}^2} F_g @ \frac{M_g^2}{m_{\tilde{b}_1}^2} A \frac{5}{3}; \quad (39)$$

where the mixing angle $\frac{R_L}{32}$ and phase $\frac{R_L}{32}$ are defined in Appendix A, and F_4 and F_g are defined in Appendix B. In the above equation, we have neglected the effect of running the \tilde{b}_1 contribution from m_0 to M_W as the \tilde{b}_2 contribution is dominant.

The dominant new physics contribution is given by adding Eqs. (37), (38) and (39), which yields

$$C_{7,8g}^{\text{new}}(M_W) = C_{7,8g}^H(M_W) + C_{7,8g}^{\tilde{t}_1}(M_W) + C_{7,8g}^g(M_W); \quad (40)$$

In what follows we will discuss in detail the new physics contribution predicted by the U(2) model to the rare decay processes $B_d \rightarrow X_s$, $B_d \rightarrow X_s g$, $B_d \rightarrow X_s \pi^+$ and $B_d \rightarrow K_s$.

B. $B_d \rightarrow X_s$, $B_d \rightarrow X_s g$

The dominant operators contributing to $B_d \rightarrow X_s$ and $B_d \rightarrow X_s g$ are O_2 , O_7 and O_{8g} . The Branching Ratio $B.R.(B_d \rightarrow X_s)$, at leading order, normalized to the semi-leptonic $B.R.(B_d \rightarrow X_c e^-)$ 10.5%, is given by [3, 27, 28]

$$\frac{(B_d \rightarrow X_s)}{(B_d \rightarrow X_c e^-)}_{(E > (1 - \epsilon) E^{\text{max}})} = \frac{6}{g(\frac{m_c}{m_b})} \frac{V_{ts} V_{tb}}{V_{cb}}^2 \mathcal{C}_7 \beta; \quad (41)$$

where $g(z) = 1 - 8z + 8z^6 - z^8 - 24z^4 \ln(z)$ is a phase space function, and β is the fractional energy cut, i.e., only photon energy $E > (1 - \epsilon) E^{\text{max}}$ is accepted.

The CP asymmetry in $B_d \rightarrow X_s$ is given by [28]

$$A_{CP}^{B_d \rightarrow X_s}(\beta) = \frac{(B_d \rightarrow X_s) - (B_d \rightarrow X_s)}{(B_d \rightarrow X_s) + (B_d \rightarrow X_s)} \Big|_{E > (1 - \epsilon)E_{max}}; \\ = \frac{1}{C_7} f a_{27}(\beta) \text{Im}[C_2 C_7] + a_{87}(\beta) \text{Im}[C_{8g} C_7] + a_{28}(\beta) \text{Im}[C_2 C_{8g}] g; \quad (42)$$

For $\beta = 0.15$, which is a typical experimental cut, we use $a_{27} = 0.0124$, $a_{87} = 0.0952$ and $a_{28} = 0.0004$ [28].

The experimentally measured [17] branching ratio is $B.R.(B_d \rightarrow X_s) = (3.52^{+0.3}_{-0.28}) \cdot 10^{-4}$. In the SM, we have $C_2^{SM} = 1.11$, $C_7^{SM} = 0.31$ and $C_{8g}^{SM} = 0.15$. The SM prediction for $B.R.(B_d \rightarrow X_s)$, which depends on C_7 , is constrained by this branching ratio. In the context of SUSY this has been analyzed, for example, in Ref. [5, 23, 29].

The SM CP asymmetry in $B_d \rightarrow X_s$ is of the order of 1%, so that a larger CP asymmetry measured would imply new physics [28]. The present limit at 95% C.L. is [17, 30, 31] $0.07 < A_{CP}^{B_d \rightarrow X_s} < 0.07$.

The $B.R.(B_d \rightarrow X_s g)$ is obtained simply from Eq. (41)

$$\frac{(B_d \rightarrow X_s g)}{(B_d \rightarrow X_{ce})} = C(R) \frac{6_s}{g(\frac{m_c}{m_b})} \frac{V_{ts} V_{tb}}{V_{cb}}^2 |C_{8g}|^2; \quad (43)$$

where the SU(3) quadratic Casimir $C(R) = 4/3$. The $B.R.(B_d \rightarrow X_s g)$ has large experimental and theoretical uncertainties and Ref. [32] suggests that the data might prefer a $B.R.$ value of around 10%.

Figs. 6 and 7 show the interplay between the W , H , \tilde{g} and g contributions to $B_d \rightarrow X_s$, where the sum of these contributions to the magnitude of C_7 is constrained by $B.R.(B_d \rightarrow X_s)$. The experimental data on $B.R.(B_d \rightarrow X_s)$ allows (at 2 σ) the region bounded by the contours shown in the figures. In the plots, the parameters are as given in Table I, and some relevant ones are varied as shown in the figures.

To illustrate the dependence on the MFV parameters, we consider for example, in Fig. 6, the dependence of $A_{CP}^{B_d \rightarrow X_s}$ and $B.R.(B_d \rightarrow X_s)$ as a function of m_H and M_2 (left) and as a function of $\tan\beta$ and $\arg(\tilde{g})$ (right), for the choice of parameters shown in Table I.

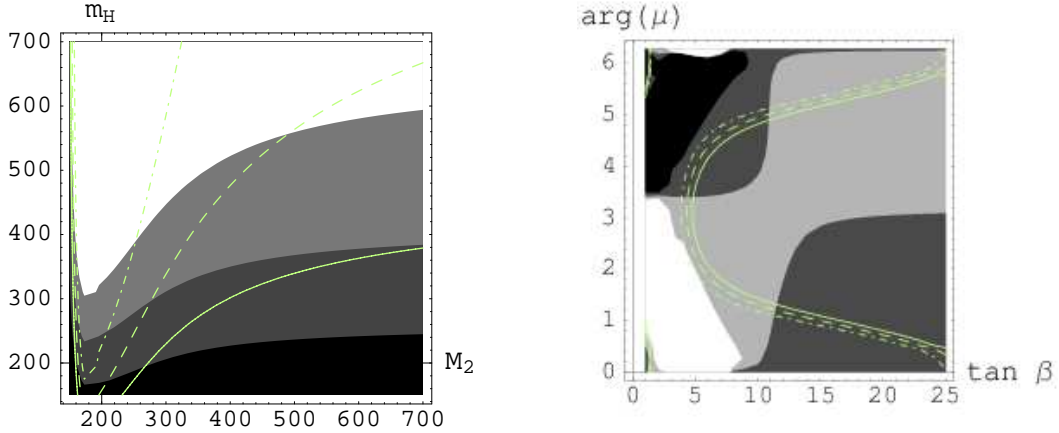


FIG . 6: The boundaries between the shaded regions show (2.5,3,3.5)% (darkest to lightest) contours of $A_{CP}^{B_d! X_s}$ as a function of m_H and M_2 (left), and, (-3.5,0,3.5)% (darkest to lightest) contours of $A_{CP}^{B_d! X_s}$ as a function of $\tan \beta$ and $\arg(\mu)$ (right). Superimposed is the experimental 2 allowed contours of $B_R.(B_d! X_s)$.

The experimental 2 allowed contours of $B_R.(B_d! X_s)$ are also shown. In Fig. 7 (left), the shaded regions show $A_{CP}^{B_d! X_s}$ as a function of the magnitude and argument of d_{32}^{RL} , the dimensionless O (1) coefficient defined in Eq (7). In Fig. 7 (right), we show contours of $B_R.(B_d! X_s)$, and a B R. of up to about 15% can be accommodated in this model.

C . $B_d! X_s^{+ \gamma}$

The dominant operators contributing to $B_d! X_s^{+ \gamma}$ ($\gamma = e, \nu$) are O_7 , O_9 and O_{10} . It is usual to define

$$C_9(\gamma) = \frac{1}{2} \tilde{C}_9(\gamma);$$

$$C_{10} = \frac{1}{2} \tilde{C}_{10};$$

and

$$S = \frac{(p_+ + p_-)^2}{m_b^2}; \quad (44)$$

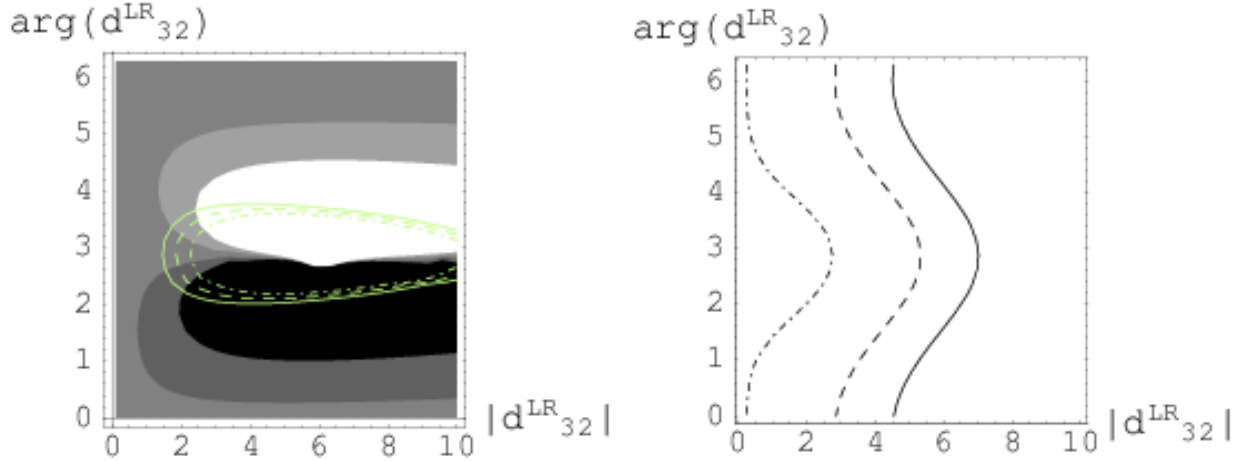


FIG . 7: The boundaries between the shaded regions show $(-7, -3, 3, 7)\%$ (darkest to lightest) contours of $A_{CP}^{B_d! X_s^+}$ (left) with experimentally allowed 2 contours of $B_d! X_s^+$ superimposed, and, 1%, 7.5% and 15% contours of predicted $B_d! X_s^+ g$ (right).

The (differential) partial width $\frac{d}{ds} (B_d! X_s^+)$, normalized to $(B_d! X_c e)$, is given by [22]:

$$R(s) \frac{\frac{d}{ds} (B_d! X_s^+)}{(B_d! X_c e)} = \frac{1}{4} \frac{V_{ts} V_{tb}}{V_{cb}}^2 \frac{(1 - \frac{s}{m_c})^h}{f(\frac{m_c}{m_b})} (1 + 2s) \frac{C_9^{\text{eff}} j^2 + C_{10} j^2}{1 + \frac{2}{s} j_7 j^2 + 12 \text{Re}(C_7 C_9^{\text{eff}})} ; \quad (45)$$

where f and j are phase space functions and C_9^{eff} is the QCD corrected C_9 , given in terms of C_9 and C_i ($i = 1 \dots 6$) [22]. Integrating this we get the prediction for the decay branching ratios and we show this in Table II for the SM along with the experimental result [17]. We choose the lower limit on the integration to correspond to a typical experimental choice, $(p_+ + p_-)^2 > (0.2 \text{ GeV})^2$. Since the rate of $B_d! X_s^+$ is down by the square of the electromagnetic coupling constant compared to $B_d! X_s$, the experimental errors are comparatively larger.

Fig. 8 shows the contours of $B_d! X_s^+$ as a function of d_{32}^{RL} . Compared to

	Experiment[17]	SM prediction
$B.R.(B_d \rightarrow X_s \pi^+ \pi^-)$	$4.46^{+0.98}_{-0.96} \times 10^{-6}$	5.3×10^{-6}

TABLE II: The current data for $B_d \rightarrow X_s \pi^+ \pi^-$.

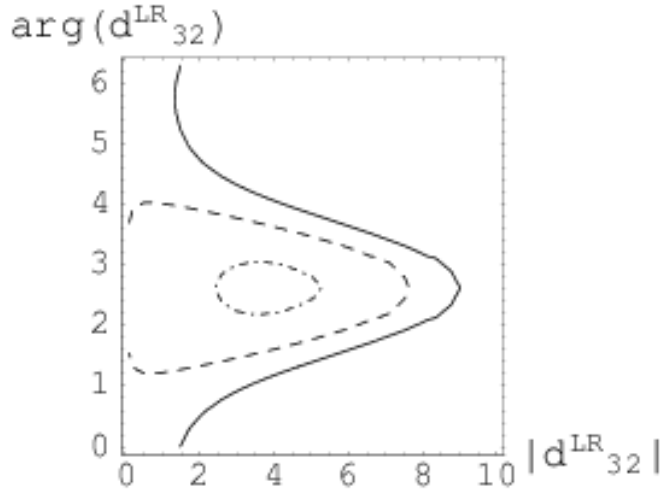


FIG. 8: The (dash-dot, dash, solid) curves are $(5.25; 6.25; 7.25) \times 10^{-6}$ contours of $B_d \rightarrow X_s \pi^+ \pi^-$.

$B.R.(B_d \rightarrow X_s)$, c.f. Fig. 7 (left), the $B_d \rightarrow X_s \pi^+ \pi^-$ constraint is not very stringent right now, and improved statistics at the B-factories could place tighter constraints on the parameter space.

D. $B_d \rightarrow K_s$

The decay $B_d \rightarrow K_s (\bar{b} \rightarrow s \bar{s} s \bar{s}$ at the quark level) can be a sensitive probe of new physics since the leading order SM contribution is one-loop suppressed, and loop processes involving heavy SUSY particles can contribute significantly. However, the computation of $B.R.(B_d \rightarrow K_s)$ suffers from significant theoretical uncertainties in calculating the hadronic

matrix elements. We follow the factorization approach, details of which are presented in Ref. [34]. The theoretical uncertainties largely cancel in the CP asymmetry, and is therefore a good probe of new physics.

The CP asymmetry in $B_d \rightarrow K_s$ is defined by

$$A_{CP}^{B_d \rightarrow K_s} = \frac{B_d(t) \bar{K}_s - \bar{B}_d(t) K_s}{B_d(t) \bar{K}_s + \bar{B}_d(t) K_s} \quad (46)$$

$$= C_K \cos(m_{B_d} t) + S_K \sin(m_{B_d} t); \quad (47)$$

where

$$\begin{aligned} C_K &= \frac{1 - j_K \frac{\partial}{\partial t}}{1 + j_K \frac{\partial}{\partial t}}; \\ S_K &= \frac{2 \operatorname{Im}(\frac{\partial}{\partial t})}{1 + j_K \frac{\partial}{\partial t}}; \\ &= e^{2i(\frac{\partial}{\partial t})} \frac{A(B_d \rightarrow K_s)}{A(B_d \rightarrow K_s)}; \end{aligned}$$

where $B_d(t)$ represents the state that is a B_d at time $t = 0$, m_{B_d} is the $B_d B_d$ mass difference, $\frac{\partial}{\partial t}$ is the usual angle in the SM CKM unitarity triangle, α is the CP asymmetry in $B_d \rightarrow K_s$, and $\frac{\partial}{\partial t}$ is any new physics contributions to $B_d B_d$ mixing ($\frac{\partial}{\partial t}$ is discussed in Section IV B). The SM predicts that the CP asymmetry in $B_d \rightarrow K_s$ and $B_d \rightarrow \bar{K}_s$ should be the same, i.e., $S_K = \sin 2\alpha$.

The $B_d \rightarrow K_s$ amplitude and partial decay width are given by [8, 34]:

$$A(B_d \rightarrow K_s) = \sum_{p=u,c}^X a_p (a_3 + a_4^p + a_5) - \frac{1}{2} (a_7 + a_9 + a_{10}^p) \quad (48)$$

$$(B_d \rightarrow K_s) = \frac{G_F^2 f^2 m_B^3}{32} (F_1^{B \rightarrow K})^2 \frac{\partial}{\partial t} A(B_d \rightarrow K_s) \frac{\partial}{\partial t} \left(1; \frac{m^2}{m_B^2}, \frac{m_K^2}{m_B^2} \right)^{\frac{3}{2}} \quad (49)$$

where the phase space function^x $(x; y; z) = x^2 + y^2 + z^2 - 2xy - 2yz - 2zx$, the decay constant $f = 237$ MeV, the form factor $F_1^{B \rightarrow K} = 0.38$ and $a_p = V_{pb} V_{ps}$. The SM a_i 's, in terms of the C_i 's, are given in Ref. [34] to which we add the new physics contribution given in Eq. (40). We do not include the power-suppressed weak annihilation operators and

^x We thank Liantao Wang for clarifying the expression for $(x; y; z)$.

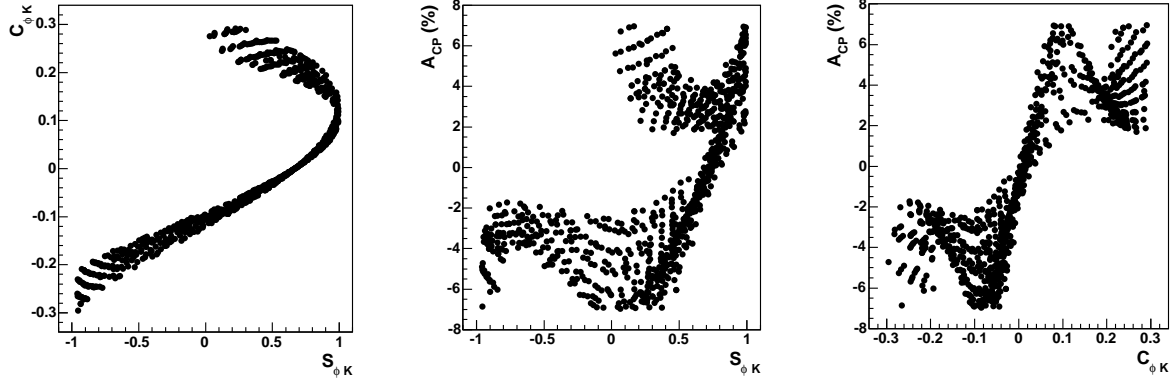


FIG. 9: $A_{CP}^{B_d \rightarrow K_s}$, S_K and C_K for points that satisfy all experimental constraints (within 2 σ), resulting from a scan over d_{32}^{LR} and $\arg(\dots)$, for small d_R s_R mixing (negligible d).

we refer the reader to Refs. [34] and [35] for a more complete discussion. As explained in Section II B, we are only including the $_{32}^{RL}$ SUSY contribution, as this is the dominant one. The amplitude for the CP conjugate process $B_d \rightarrow K_s$ is obtained by taking $_{CP}^{B_d \rightarrow K_s} = -_{CP}^{B_d \rightarrow K_s}$.

The current $B_d \rightarrow K_s$ experimental average [17] is summarized in Table III. The SM requires $S_K = S_{J=K} = \sin 2\alpha$, but the experimental data has about a 2 σ discrepancy between S_K and $S_{J=K}$.¹ Though not convincing yet, this could be an indication of new physics and we ask if this can be naturally explained in the theory we are considering.

	Experiment [17]		SM prediction	
$B \otimes (B_d \rightarrow K_s)$	$8.3^{+1.2}_{-1.0}$	10^{-6}	5	10^{-6}
S_K	0.34	0.2	0.725	0.037
C_K	0.04	0.17		0

TABLE III: The current data for $B_d \rightarrow K_s$.

We showed in Section IV B, that if d_R s_R mixing is small, there is no significant new phase in $M_{12}(B_d)$ (i.e., $d \approx 0$). For this case, we scan the parameter space $\arg(\dots)$, $j_{32}^{RL} \otimes \arg(\dots)$, and in Fig. 9 show a scatter-plot of the points that satisfy all experimental constraints

¹ The discrepancy in S with all $b \rightarrow s$ penguin modes, and S with all charm onium modes is at 3:6.

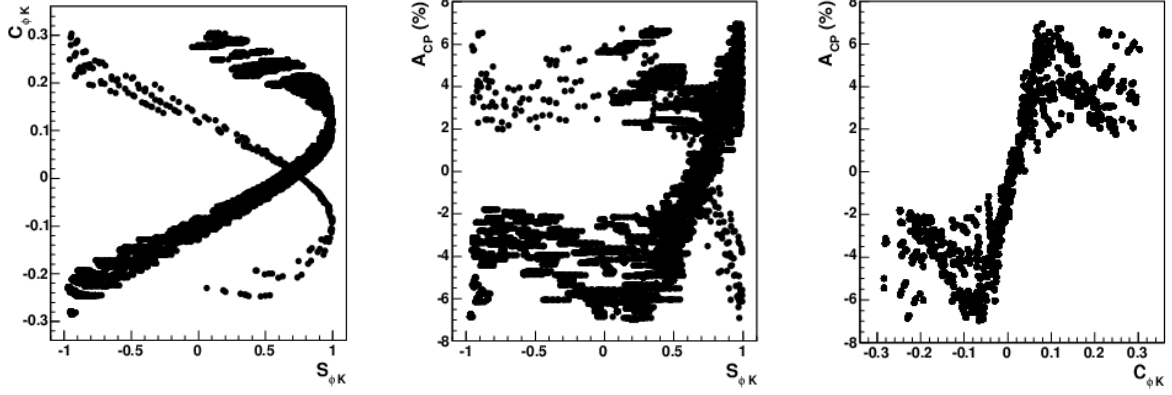


FIG. 10: $A_{CP}^{B_d \rightarrow X_s}$, S_K and C_K for points that satisfy all experimental constraints (within 2 σ), resulting from a scan over $j_{32}^{LR,RR}$ and $\arg(j)$, for large $\tilde{d}_R s_R$ mixing (nonzero \tilde{d}_d).

including $B_R(B_d \rightarrow X_s)$ and $B_R(B_d \rightarrow K_s)$. We find that it is possible to satisfy all experimental constraints including the recent $B_d \rightarrow K_s$ data shown in Table III in the framework we are considering. Furthermore, there are strong correlations between $A_{CP}^{B_d \rightarrow X_s}$, S_K and C_K . As the accuracy of the experimental data improve, we can use these correlations to (in)validate the choices that we make in our model.

Large $\tilde{d}_R s_R$ mixing can lead to a nonzero \tilde{d}_d which depends on $j_{32}^{RR} j$ as explained in Section IV B. We therefore include this new phase and perform a scan over $j_{32}^{RR} j$, $\arg(j_{32}^{RR})$, $\arg(j)$, $j_{32}^{RL} j$ and $\arg(j_{32}^{RL})$. We show the points that satisfy all experimental constraints and the resulting $A_{CP}^{B_d \rightarrow X_s}$, S_K and C_K in Fig. 10. We again see from Fig. 10 that $A_{CP}^{B_d \rightarrow X_s}$, S_K and C_K are strongly correlated, although the effect of the new phase in $B_d B_d$ mixing allows new regions of parameter space compared to the small mixing case shown in Fig. 9. Even in the case of large mixing we find that it is possible to satisfy all experimental data including the S_K and C_K . One feature that we find in either large or small mixing case is that sign (C_K) is positively correlated with sign ($A_{CP}^{B_d \rightarrow X_s}$). Thus, further data could shed light on the validity of the choices that we make in our model.

VI. CONCLUSIONS

A supersymmetric $U(2)$ theory has the potential to explain the gauge hierarchy and flavor problems in the SM. We assumed an effective SUSY mass spectrum just above the weak scale, the only relatively light scalars being the right handed stop and sbottom (weak scale masses). We analyzed what such a hypothesis would imply for K and B meson observables by including all the dominant contributions that can interfere in a certain observable. Although for definiteness we considered a $U(2)$ framework, our conclusions hold for any theory with a similar SUSY mass spectrum and structure of the squark mass matrix.

The CP violation parameter in Kaon mixing, ϵ_K , can impose constraints on the MFV parameter space of our model, as we showed in Fig. 2, while the gluino contribution to ϵ_K is negligible. There is sufficient room to accommodate the MFV contributions to ϵ_K , given the present uncertainty in the lattice computation of the Bag parameter B_K .

We find that $B_d B_d$ mixing and $\epsilon_{K_s} (\sin 2\beta)$ can impose constraints on the supersymmetric $U(2)$ theory. In addition to the MFV contribution, if $\tilde{d}_R \tilde{s}_R$ mixing is large, the gluino contributions to $B_d B_d$ mixing can be significant leading to a strong constraint on the 32 entry of the RR squark mass matrix, \tilde{m}_{32}^{RR} , as shown in Fig. 4. Furthermore, in this case, there is a new phase in the $B_d B_d$ mixing amplitude coming from the SUSY sector. However, if $\tilde{d}_R \tilde{s}_R$ mixing is small, the constraint on \tilde{m}_{32}^{RR} from $B_d B_d$ mixing is weak.

$B_s B_s$ mixing most sensitively depends on \tilde{m}_{32}^{RR} in the SUSY $U(2)$ theory. If \tilde{m}_{32}^{RR} is unconstrained by $B_d B_d$ mixing (small $\tilde{d}_R \tilde{s}_R$ mixing), we showed that m_{B_s} can be increased to quite large values (up to about 40 ps^{-1}), c.f. Fig. 5. The current and upcoming experiments can reach sensitivities required to see the SM prediction for m_{B_s} . Seeing a higher value, or not seeing a signal at all, might hint at some new physics of the type we are considering. We also presented expectations for the B_s dilepton asymmetry, $A_{ll}^{B_s}$, which can constrain \tilde{m}_{32}^{RR} .

The experimental data on $B_R(B_d \rightarrow X_s)$ imposes a constraint on the SUSY theory. While satisfying this constraint, we showed that an enhancement in CP violation in $B_d \rightarrow X_s$

X_s is possible. Since in the SM, $A_{CP}^{B_d! X_s}$ is predicted to be less than 1%, if a much larger value is measured, it would clearly point to new physics. In Fig. 7 we presented the expectations for $A_{CP}^{B_d! X_s}$ and $B_R(B_d! X_s)$ while varying the magnitude and phase of $_{32}^{RL}$. We also presented expectations for $B_R(B_d! X_s^{+})$ in Fig. 8.

The present experimental data on the CP violation in $B_d! K_s$ has about a 2 deviation from the SM prediction, and it will be very interesting to see if this would persist with more data. We showed that such a deviation can be accommodated in the framework we are considering, both for large or small $\alpha_R s_R$ mixing. We showed, in Fig. 10, that $A_{CP}^{B_d! X_s}$ can be enhanced significantly while satisfying all other experimental bounds including the present data on S_K and C_K . In Figs. 9 and 10, for small and large $\alpha_R s_R$ mixing respectively, we see strong correlations between $A_{CP}^{B_d! X_s}$, S_K and C_K . Comparing these with upcoming data with improved precision could shed light on the validity of the choices that we make in our model.

We conclude by remarking that the prospects are exciting for discovering SUSY in B -meson processes at current and upcoming colliders. Here, we showed this for a SUSY $U(2)$ model. To unambiguously establish that it is a SUSY $U(2)$ theory, and to determine the various SUSY breaking parameters, will require looking at a broad range of observables.

Acknowledgments

We thank P. Ko, U. Nierste, K. Tobe, J. Wells and M. Whisnant for many stimulating discussions, and, D. Bortoletto and C. Rott for discussions on the Tevatron bounds. CPY thanks the hospitality of the National Center for Theoretical Sciences in Taiwan, ROC, where part of this work was completed. SG acknowledges support from the high energy physics group at Northwestern University where this work was completed. This work was supported in part by the NSF grant PHY-0244919.

A P P E N D I X A : M IX IN G A N G L E S

The charged SU (2) Majorana gauginos \tilde{W}_1, \tilde{W}_2 can be combined to form the Dirac spinor

$$\tilde{W}^+ = \frac{1}{2} \begin{pmatrix} \tilde{W}_1^+ \\ \tilde{W}_2^+ \end{pmatrix} ; \quad (A 1)$$

where $\tilde{W}^+ = \tilde{W}_1^+ + \tilde{W}_2^+$. The up and down type Higgsinos can be combined to form the Dirac spinor

$$\tilde{H}^+ = \begin{pmatrix} \tilde{H}_u^+ \\ \tilde{H}_d^+ \end{pmatrix} ; \quad (A 2)$$

The chargino mass terms can then be written as

$$L = \overline{\tilde{W}^+} \overline{\tilde{H}^+} (M_P P_L + M^Y P_R) \begin{pmatrix} \tilde{W}^+ \\ \tilde{H}^+ \end{pmatrix} ; \quad (A 3)$$

where

$$M = \frac{p}{2} \begin{pmatrix} M_2 & \frac{p}{2} \sin m_W \\ \frac{p}{2} \cos m_W & \end{pmatrix} ; \quad (A 4)$$

We can go to the chargino mass eigen basis $(\tilde{\chi}_1^+, \tilde{\chi}_2^+)$ by making the rotations

$$\begin{pmatrix} \tilde{W}^+ \\ \tilde{H}^+ \end{pmatrix} = (C_{L,R}) \begin{pmatrix} \tilde{\chi}_1^+ \\ \tilde{\chi}_2^+ \end{pmatrix} ; \quad (A 5)$$

with the rotation matrices $C_{L,R}$ given as

$$C = \begin{pmatrix} \cos & \sin e^{i\alpha} & e^{i\beta} & 0 \\ \sin e^{i\alpha} & \cos & 0 & e^{i\beta} \end{pmatrix} ; \quad (A 6)$$

where the mixing angles and phases are [25]

$$\begin{aligned} \alpha_L &= \arg(M_2 + \cot \beta) \\ \tan 2\alpha_L &= \frac{p \frac{8m_W}{2} \sin \beta M_2 + \cot \beta}{M_2^2 + j \frac{2m_W^2}{2} \cos 2\beta} \\ \alpha_R &= \arg(M_2 + \tan \beta) \\ \tan 2\alpha_R &= \frac{p \frac{8m_W}{2} \cos \beta M_2 + \tan \beta}{M_2^2 - j \frac{2m_W^2}{2} \cos 2\beta} \\ \beta_R &= \arg C_R (M_2 C_L + \frac{p}{2m_W} \sin s_L e^{i\alpha_L}) + s_R e^{i\beta_R} (\frac{p}{2m_W} \cos c_L + s_L e^{i\alpha_L}) \\ \beta_R &= \arg C_R (\frac{p}{2m_W} \cos s_L e^{i\alpha_L} - c_L) + s_R e^{i\beta_R} (-M_2 s_L e^{i\alpha_L} + \frac{p}{2m_W} \sin c_L) \end{aligned} \quad (A 7)$$

with 0 = 2 so that $M_1^2 > M_2^2$, and, $s_{L,R} = \sin_{L,R}$ and $c_{L,R} = \cos_{L,R}$.

The sbottom mass terms are given as, c.f. Eq. (5)

$$L \quad (\tilde{b}_L \quad \tilde{b}_R) \quad \begin{matrix} m_{3L}^2 + m_b^2 + \frac{d_L}{L} (v_d A_b \quad \tan m_b) \\ v_d A_b \quad \tan m_b \quad m_{\tilde{b}_R}^2 + m_b^2 + \frac{d_R}{R} \end{matrix} \quad \begin{matrix} ! \quad \tilde{b}_L \\ \tilde{b}_R \end{matrix} ; \quad (A 8)$$

where the L,R are the D-term contributions given as

$$d = T_3 Q_{EM} \sin^2 \theta_W \cos 2 \theta_Z^2 : \quad (A 9)$$

This is diagonalized by the rotation

$$(\tilde{b}_L \quad \tilde{b}_R) \quad \begin{matrix} ! \quad \cos \beta \quad \sin \beta e^{i\beta} \\ \tilde{b}_L \quad \tilde{b}_R \quad \sin \beta e^{i\beta} \quad \cos \beta \\ \tilde{b}_1 \quad \tilde{b}_2 \\ \tilde{b}_1 \quad \tilde{b}_2 \end{matrix} ; \quad (A 10)$$

where the mixing angle and phase are given by

$$\tan 2\beta = \frac{2v_d A_b}{(m_3^2 + \frac{d_L}{L})} \frac{\tan m_b}{(m_{\tilde{b}_R}^2 + \frac{d_R}{R})} ;$$

$$\beta = \arg(v_d A_b \quad \tan m_b) : \quad (A 11)$$

We have similar equations for stop mixing with obvious changes in addition to the off-diagonal term now being given as: $(v_u A_t \quad \cot m_t)$. In our framework, owing to the smallness of the off-diagonal RL mixing term compared to $m_3^2 \quad m_0^2$, we have negligible stop and sbottom mixing so that we neglect their effects. We thus have $\tilde{b}_1 = \tilde{b}_L$ and $\tilde{b}_2 = \tilde{b}_R$ and similarly for the stop.

To compute the interaction vertices in the SuperKM basis, one could diagonalize the 6x6 squark mass matrix. Since the off-diagonal entries in our case are small, we perform an approximate leading order diagonalization of the mass matrices shown in Eq. (5).

Focusing first on the \tilde{b}_R s_L mixing,

$$L \quad (\tilde{b}_L \quad \tilde{b}_R) \quad \begin{matrix} m_{1LL}^2 + m_{2LL}^2 + m_s^2 + \frac{d_L}{L} (v_d A_4^0) \\ v_d A_4^0 \end{matrix} \quad \begin{matrix} ! \quad s_L \\ \tilde{b}_R \end{matrix} : \quad (A 12)$$

This is diagonalized by the rotation

$$\begin{aligned}
 \mathbf{s}_L &= \begin{pmatrix} \cos \frac{R_L}{32} & \sin \frac{R_L}{32} e^{i \frac{R_L}{32}} \\ \sin \frac{R_L}{32} e^{-i \frac{R_L}{32}} & \cos \frac{R_L}{32} \end{pmatrix} \begin{pmatrix} \mathbf{q}_2 \\ \mathbf{q}_3 \end{pmatrix} \\
 \tilde{\mathbf{b}}_R &= \begin{pmatrix} \cos \frac{R_L}{32} & \sin \frac{R_L}{32} e^{i \frac{R_L}{32}} \\ \sin \frac{R_L}{32} e^{-i \frac{R_L}{32}} & \cos \frac{R_L}{32} \end{pmatrix} \begin{pmatrix} \mathbf{q}_2 \\ \mathbf{q}_3 \end{pmatrix} \\
 C_{\tilde{\mathbf{b}}_R \mathbf{s}_L} &= \begin{pmatrix} \mathbf{q}_2 \\ \mathbf{q}_3 \end{pmatrix} : \quad (A 13)
 \end{aligned}$$

The mixing angle and phase are given by

$$\begin{aligned}
 \tan 2 \frac{R_L}{32} &= \frac{2 j v_d A}{(m_{1LL}^2 + m_s^2 + \frac{d}{L}) (m_{\tilde{b}_R}^2 + m_b^2 + \frac{d}{R})} ; \\
 \frac{R_L}{32} &= \arg(v_d A) : \quad (A 14)
 \end{aligned}$$

The $\tilde{\mathbf{b}}_R \mathbf{s}_R$ mixing is given similarly. We have the mass terms

$$\begin{aligned}
 L & \quad (\mathbf{s}_L \tilde{\mathbf{b}}_R) \begin{pmatrix} m_{1RR}^2 + m_s^2 + \frac{d}{R} & (m_4^2) \\ m_4^2 & m_{\tilde{b}_R}^2 + m_b^2 + \frac{d}{R} \end{pmatrix} \begin{pmatrix} \mathbf{q}_2 \\ \mathbf{q}_3 \end{pmatrix} ; \quad (A 15)
 \end{aligned}$$

which is diagonalized by the rotation

$$\begin{aligned}
 \mathbf{s}_R &= \begin{pmatrix} \cos \frac{R_R}{32} & \sin \frac{R_R}{32} e^{i \frac{R_R}{32}} \\ \sin \frac{R_R}{32} e^{-i \frac{R_R}{32}} & \cos \frac{R_R}{32} \end{pmatrix} \begin{pmatrix} \mathbf{q}_2 \\ \mathbf{q}_3 \end{pmatrix} \\
 \tilde{\mathbf{b}}_R &= \begin{pmatrix} \cos \frac{R_R}{32} & \sin \frac{R_R}{32} e^{i \frac{R_R}{32}} \\ \sin \frac{R_R}{32} e^{-i \frac{R_R}{32}} & \cos \frac{R_R}{32} \end{pmatrix} \begin{pmatrix} \mathbf{q}_2 \\ \mathbf{q}_3 \end{pmatrix} \\
 C_{\tilde{\mathbf{b}}_R \mathbf{s}_R} &= \begin{pmatrix} \mathbf{q}_2 \\ \mathbf{q}_3 \end{pmatrix} : \quad (A 16)
 \end{aligned}$$

The mixing angle and phase are given by

$$\begin{aligned}
 \tan 2 \frac{R_R}{32} &= \frac{2 j m_4^2 j}{(m_{1RR}^2 + m_s^2 + \frac{d}{R}) (m_{\tilde{b}_R}^2 + m_b^2 + \frac{d}{R})} ; \\
 \frac{R_R}{32} &= \arg(m_4^2) : \quad (A 17)
 \end{aligned}$$

The $\tilde{\mathbf{d}}_L \mathbf{s}_L$ and $\tilde{\mathbf{d}}_R \mathbf{s}_R$ mixing terms are

$$\begin{aligned}
 L & \quad (\tilde{\mathbf{d}}_L \mathbf{s}_L \tilde{\mathbf{d}}_R \mathbf{s}_R) \begin{pmatrix} m_1^2 + m_d^2 + \frac{d}{L,R} & i \mathbf{m}_5^2 \\ i \mathbf{m}_5^2 & m_1^2 + m_s^2 + 2m_2^2 + \frac{d}{L,R} \end{pmatrix} \begin{pmatrix} \mathbf{q}_1 \\ \mathbf{q}_2 \end{pmatrix} : \quad (A 18)
 \end{aligned}$$

The matrices that diagonalizes these, $C_{\tilde{\mathbf{d}}_L \mathbf{s}_L}$ and $C_{\tilde{\mathbf{d}}_R \mathbf{s}_R}$ are given analogous to Eq. (A 16), the angle and phase ($\frac{LL}{12}, \frac{LL}{12}$) and ($\frac{RR}{12}, \frac{RR}{12}$) given analogous to Eq. (A 17), and we will not write them down explicitly. The diagonal entries are split only by 0 (2), and therefore this mixing is maximal in general. However, if $\mathbf{m}_5^2 = 2m_2^2$, this mixing can be small.

The $B_d \rightarrow X_s$ loop functions are given by

$$\begin{aligned}
 F_7^{LL}(x) &= \frac{x(7 - 5x - 8x^2)}{36(x - 1)^3} + \frac{x^2(3x - 2)}{6(x - 1)^4} \ln x \quad ; \\
 F_8^{LL}(x) &= \frac{x(2 + 5x - x^2)}{12(x - 1)^3} \quad \frac{3x^2}{6(x - 1)^4} \ln x \quad ; \\
 F_7^{RL}(x) &= \frac{5 - 7x}{6(x - 1)^2} + \frac{x(3x - 2)}{3(x - 1)^3} \ln x \quad ; \\
 F_8^{RL}(x) &= \frac{1 + x}{2(x - 1)^2} \quad \frac{x}{(x - 1)^3} \ln x \quad ; \\
 F_7^{RL}(x) &= \frac{x(3 - 5x)}{12(x - 1)^2} + \frac{x(3x - 2)}{6(x - 1)^3} \ln x \quad ; \\
 F_8^{RL}(x) &= \frac{x(3 - x)}{4(x - 1)^2} \quad \frac{x}{2(x - 1)^3} \ln x \quad ; \tag{B1}
 \end{aligned}$$

$$\begin{aligned}
 F_4(x) &= \frac{x^2 - 1 - 2x \ln x}{2(x - 1)^3} \\
 F_9(x) &= \frac{5x^2 - 18x + 13 + (9 - x) \ln x}{3(x - 1)^3} \tag{B2}
 \end{aligned}$$

The SM box functions are given by

$$\begin{aligned}
 S_0(x) &= \frac{4x - 11x^2 + x^3}{4(1 - x)^2} \quad \frac{3x^3 \ln x}{2(1 - x)^3} \quad ; \\
 S_0(x_1, x_2) &= \frac{x_1 x_2}{4} \quad \frac{x_1^2 - 8x_1 + 4}{(x_1 - x_2)(x_1 - 1)^2} \ln x_1 + \frac{x_2^2 - 8x_2 + 4}{(x_2 - x_1)(x_2 - 1)^2} \ln x_2 \\
 &\quad \frac{3}{(x_1 - 1)(x_2 - 1)} \quad : \tag{B3}
 \end{aligned}$$

The charged-Higgs and chargino box functions are given by

$$\begin{aligned}
 Y_1(r; r; s_i; s_j) &= \frac{r^2}{(r - r)(s_i - r)(s_j - r)} \ln r + \frac{r^2}{(r - r)(s_i - r)(s_j - r)} \ln r \\
 &\quad + \frac{s_i^2}{(r - s_i)(r - s_i)(s_j - s_i)} \ln s_i + \frac{s_j^2}{(r - s_j)(r - s_j)(s_i - s_j)} \ln s_j ; \\
 Y_2(r; r; s_i; s_j) &= \frac{P}{s_i s_j} \quad \frac{r}{(r - r)(s_i - r)(s_j - r)} \ln r + \frac{r}{(r - r)(s_i - r)(s_j - r)} \ln r \\
 &\quad + \frac{s_i}{(r - s_i)(r - s_i)(s_j - s_i)} \ln s_i + \frac{s_j}{(r - s_j)(r - s_j)(s_i - s_j)} \ln s_j \tag{B4}
 \end{aligned}$$

from which various limiting cases can be obtained.

The gluino box integrals are given as

$$\begin{aligned} I_4 &= I_4(M_g^2; M_g^2; m_{b_R}^2; m_{b_R}^2) = \frac{Z}{(2\pi)^4} \frac{d^4 p}{(p^2 - M_g^2)(p^2 - M_g^2)(p^2 - m_{b_R}^2)(p^2 - m_{b_R}^2)}; \\ I_4' &= I_4'(M_g^2; M_g^2; m_{b_R}^2; m_{b_R}^2) = \frac{Z}{(2\pi)^4} \frac{d^4 p}{(p^2 - M_g^2)(p^2 - M_g^2)(p^2 - m_{b_R}^2)(p^2 - m_{b_R}^2)}; \end{aligned} \quad (B5)$$

which we evaluate numerically using LoopTools [38] in Mathematica.

- [1] A. G. Cohen, D. B. Kaplan and A. E. Nelson, "The more minimal supersymmetric standard model," *Phys. Lett. B* 388, 588 (1996) [[hep-ph/9607394](#)].
- [2] A. Pomarol and D. Tommasini, "Horizontal symmetries for the supersymmetric flavor problem," *Nucl. Phys. B* 466, 3 (1996) [[hep-ph/9507462](#)].
- [3] R. Barbieri, G. R. Dvali and L. J. Hall, "Predictions From A U(2) Flavour Symmetry In Supersymmetric Theories," *Phys. Lett. B* 377, 76 (1996) [[hep-ph/9512388](#)]; R. Barbieri, L. J. Hall and A. Romano, "Consequences of a U(2) flavor symmetry," *Phys. Lett. B* 401, 47 (1997) [[hep-ph/9702315](#)].
- [4] G. Degrassi, P. Gambino and G. F. Giudice, "B → X/s gamma in supersymmetry: Large contributions beyond the leading order," *JHEP* 0012, 009 (2000) [[hep-ph/0009337](#)]; M. Carena, D. Garcia, U. Nierste and C. E. Wagner, "b → s gamma and supersymmetry with large tan(beta)," *Phys. Lett. B* 499, 141 (2001) [[hep-ph/0010003](#)].
- [5] S. Bertolini, F. Borzumati, A. Masiero and G. Ridolfi, "Effects Of Supergravity Induced Electroweak Breaking On Rare Decays And Mixings," *Nucl. Phys. B* 353, 591 (1991).
- [6] J. S. Hagelin, S. Kelley and T. Tanaka, "Supersymmetric flavor changing neutral currents: Exact amplitudes and phenomenological analysis," *Nucl. Phys. B* 415, 293 (1994).
- [7] L. J. Hall, V. A. Kostelecky and S. Raby, "New Flavor Violations In Supergravity Models," *Nucl. Phys. B* 267, 415 (1986); F. Gabbiani and A. Masiero, "FCNC In Generalized Supersymmetric Theories," *Nucl. Phys. B* 322, 235 (1989); F. Gabbiani, E. Gabrielli, A. Masiero and L. Silvestrini, "A complete analysis of FCNC and CP constraints in general

SUSY extensions of the standard model," *Nucl. Phys. B* 477, 321 (1996) [[hep-ph/9604387](#)]; M. Misiak, S. Pokorski and J. Rosiek, "Supersymmetry and FCNC effects," *Adv. Ser. Direct. High Energy Phys.* 15, 795 (1998) [[hep-ph/9703442](#)].

[8] G. L. Kane, P. Ko, H. b. Wang, C. Kolda, J. H. Park and L. T. Wang, "B/d ! PhiK (S) and supersymmetry," [[hep-ph/0212092](#)].

[9] T. A. older et al. [CDF Collaboration], "Search for scalar top and scalar bottom quarks in p anti-p collisions at *Phys. Rev. Lett.* 84, 5704 (2000) [[hep-ex/9910049](#)]; C. Rott, "Searches for the Supersymmetric Partner of the Bottom Quark," [[hep-ex/0410007](#)].

[10] S. Eidelman et al. [Particle Data Group Collaboration], "Review of particle physics," *Phys. Lett. B* 592, 1 (2004).

[11] G. Buchalla, A. J. Buras and M. E. Lautenbacher, "Weak Decays Beyond Leading Logarithms," *Rev. Mod. Phys.* 68, 1125 (1996) [[hep-ph/9512380](#)].

[12] G. C. Branco, G. C. Cho, Y. Kizukuri and N. Oshimo, "Supersymmetric contributions to B0 - anti-B0 and K0 - anti-K0 mixings," *Phys. Lett. B* 337, 316 (1994) [[hep-ph/9408229](#)]; "Searching for signatures of supersymmetry at B factories," *Nucl. Phys. B* 449, 483 (1995).

[13] D. Becirevic et al., "B/d anti-B/d mixing and the B/d ! J/psi K (S) asymmetry in general SUSY models," *Nucl. Phys. B* 634, 105 (2002) [[hep-ph/0112303](#)].

[14] A. J. Buras and R. Fleischer, "Quark mixing, CP violation and rare decays after the top quark discovery," *Adv. Ser. Direct. High Energy Phys.* 15, 65 (1998) [[hep-ph/9704376](#)].

[15] P. Ko, J. h. Park and G. Krammer, "B0 - anti-B0 mixing, B ! J/psi K (S) and B ! X/d gamma in general MSSM," *Eur. Phys. J. C* 25, 615 (2002) [[hep-ph/0206297](#)].

[16] L. Randall and S. f. Su, "CP violating lepton asymmetries from B decays and their implication for supersymmetric flavor models," *Nucl. Phys. B* 540, 37 (1999) [[hep-ph/9807377](#)].

[17] We use the (ICHEP 2004) average from CLEO, BaBar and Belle compiled by the Heavy Flavor Averaging group. <http://www.slac.stanford.edu/xorg/hfag/>

[18] Y. Grossman, Y. Nir and M. P. Warah, "A model independent construction of the unitarity triangle," *Phys. Lett. B* 407, 307 (1997) [[hep-ph/9704287](#)].

[19] G. C. Branco, L. Lavoura and J. P. Silva, "CP Violation," *Clarendon Press, Oxford* (1999).

[20] K. Anikeev et al., "B physics at the Tevatron: Run II and beyond," [[hep-ph/0201071](#)].

[21] A. J. Buras, "Weak Hamiltonian, CP violation and rare decays," [hep-ph/9806471].

[22] A. J. Buras and M. Münz, "Effective Hamiltonian for $B \rightarrow X(s) e^+ e^-$ beyond leading logarithms in the NDR and HV schemes," Phys. Rev. D 52, 186 (1995) [hep-ph/9501281].

[23] A. J. Buras, M. Misiak, M. Münz and S. Pokorski, "Theoretical Uncertainties And Phenomenological Aspects Of $B \rightarrow X(S)$ Gamma Decay," Nucl. Phys. B 424, 374 (1994) [hep-ph/9311345].

[24] B. Grinstein, R. P. Springer and M. B. Wise, "Effective Hamiltonian For Weak Radiative B Meson Decay," Phys. Lett. B 202, 138 (1988).

[25] D. A. Demir and K. A. Olive, "B \rightarrow s gamma in supersymmetry with explicit CP violation," Phys. Rev. D 65, 034007 (2002) [hep-ph/0107329].

[26] R. Barbieri and G. F. Giudice, "b \rightarrow s gamma decay and supersymmetry," Phys. Lett. B 309, 86 (1993) [hep-ph/9303270].

[27] A. Ali, H. A. Satrian and C. Greub, "Inclusive decay rate for $B \rightarrow X/d + \gamma$ in next-to-leading logarithmic order and CP asymmetry in the standard model," Phys. Lett. B 429, 87 (1998) [hep-ph/9803314]; A. L. Kagan and M. Neubert, "QCD anatomy of $B \rightarrow X/s$ gamma decays," Eur. Phys. J. C 7, 5 (1999) [hep-ph/9805303].

[28] A. L. Kagan and M. Neubert, "Direct CP violation in $B \rightarrow X/s$ gamma decays as a signature of new physics," Phys. Rev. D 58, 094012 (1998) [hep-ph/9803368].

[29] S. Bertolini, F. Borzumati and A. Masiero, "Supersymmetric Enhancement Of Noncharmed B Decays," Nucl. Phys. B 294, 321 (1987); R. Barbieri and G. F. Giudice, "b \rightarrow s gamma decay and supersymmetry," Phys. Lett. B 309, 86 (1993) [hep-ph/9303270]; P. L. Cho, M. Misiak and D. Wyler, "K_L $\rightarrow 0e + e^-$ and $B \rightarrow X_s^- + \gamma$ Decay in the MSSM," Phys. Rev. D 54, 3329 (1996) [hep-ph/9601360]. J. L. Hewett and J. D. Wells, "Searching for supersymmetry in rare B decays," Phys. Rev. D 55, 5549 (1997) [hep-ph/9610323].

[30] S. Nishida et al. [Belle Collaboration], "Measurement of the CP asymmetry in $B \rightarrow X/s$ gamma," Phys. Rev. Lett. 93, 031803 (2004) [hep-ex/0308038].

[31] B. Aubert et al. [BABAR Collaboration], "Measurement of the direct CP asymmetry in $b \rightarrow s$ gamma decays," Phys. Rev. Lett. 93, 021804 (2004) [hep-ex/0403035].

[32] A. L. Kagan and J. Rathsman, "Hints for enhanced b $\rightarrow s$ from charm and kaon counting,"

[hep-ph/9701300].

[33] J. K. Aneko et al. [Belle Collaboration], 'Measurement of the electroweak penguin process $B^+ \rightarrow s \bar{s} l^+ l^-$ ', *Phys. Rev. Lett.* **90**, 021801 (2003) [hep-ex/0208029].

[34] M. Beneke, G. Buchalla, M. Neubert and C. T. Sachrajda, 'QCD factorization in $B^+ \rightarrow K^- \pi^+$ decays and extraction of Wolfenstein parameters', *Nucl. Phys. B* **606**, 245 (2001) [hep-ph/0104110].

[35] M. Beneke and M. Neubert, 'QCD factorization for $B^+ \rightarrow P P$ and $B^+ \rightarrow P V$ decays', *Nucl. Phys. B* **675**, 333 (2003) [hep-ph/0308039].

[36] B. Aubert et al. [BABAR Collaboration], 'Measurement of $\sin(2\beta)$ in $B^0 \rightarrow \bar{K}^0 S$ (B^-)', hep-ex/0207070.

[37] K. Abe et al. [Belle Collaboration], 'An improved measurement of mixing-induced CP violation in the neutral B meson system', hep-ex/0207098.

[38] T. Hahn and M. Perez-Victoria, 'Automatized one-loop calculations in four and D dimensions', *Comput. Phys. Commun.* **118**, 153 (1999) [hep-ph/9807565].